

# ESTIMATION OF CURRENT VECTORS IN THE EAST SEA BASED ON P-VECTOR METHOD WITH CLIMATOLOGICAL KODC, GDEM, WOA DATASETS

**Ro Y.J., Smirnov S.V., Choi Y.H.**

Chungnam National, University, Taejon, Korea

## **Introduction**

The East (Japan) Sea is drawing keen international attentions from broad spectrum of scientists, diplomats, and defense officers for its geopolitical situation, peculiar scientific assets recognized as miniature ocean for its basin-wide circulation pattern, boundary currents, polar front, meso-scale eddy activities and deep water formation. In order to understand oceanographic phenomena occurring in the East Sea, it is prerequisite to understand the physical conditions such as currents and circulation of sea water.

The circulation pattern in the East (Japan) Sea has been of major interest for its peculiar gyre, a western boundary current and its separation (Uda, 1934; Moriyasu, 1972; Yurasov & Yarichin, 1991; Sekine, 1991; Kim, 1996; Kang, 1997; Kim & Yoon, 1996; KORDI, 1987, 1999) that resembles the currents such as Kuroshio and Gulf Stream. In relation to the gyre system in the East Sea, the formation of the East Korea Warm Current (EKWC) has brought up many numerical experiments (Kawabe, 1982a and 1982b; Yoon, 1982a and 1982b; Seung, 1992; Seung & Nam, 1992; Wang *et al.*, 1999). The branching mechanism of the Tsushima Warm Current (TWC) (Kim & Legekis, 1987) has also been of interest in association with the formation of the EKWC. Recent field observations provide a new evidence of the two components of the TWC, *i.e.*, in – and off-shore ones (Hase & Yoon, 1999). Numerical experiments (Ro, 1999a) suggested a new idea to explain the formation of the EKWC in that the potential energy supply into the Ulleung basin from the meso-scale eddy is a key process. This is closely linked to the baroclinic instability and the meandering of offshore component of Tsushima Warm Current. The most prominent feature readily recognizable on the AVHRR imagery is the polar front existing between warm and cold water masses in the south and north of approximate 39°N. The formation of the polar front is a key to understanding of the circulation gyre in the entire basin, since it is closely related to current system involving the TWC, EKWC, NKCC, Liman/Primorye Currents.

Information with regard to current vectors in the entire basin of the East Sea is extremely difficult to obtain, unless we resort to numerical modeling simulation. However, modeling works themselves are also subject to careful calibration and validation. The *P*-vector method recently developed to estimate the absolute geostrophic velocity from traditional hydrographic data appears to be a reliable method for this purpose.

The objectives of this study are as follows:

- 1) To obtain current vectors in time (monthly) and 3-D (horizontal and standard depths) space in the East Sea by applying the *P*-vector inversion method to climatological hydrographic datasets;
- 2) To assess the estimates of current vectors in the context of the general circulation pattern;
- 3) To compare the results of current vector estimates from different datasets;
- 4) Finally, to set up the database for the initial conditions to be used in future numerical modelling works and for model data assimilation.

## **Datasets and Method**

### Datasets

At present, two well-gridded datasets such as Generalized Digital Environmental Model (GDEM) and high resolution version of World Ocean Atlas (WOA) exist for the total basin of the East Sea. GDEM is monthly while WOA is only for annual mean. For the southwestern part of the East Sea, 27-year hydrographic datasets from Korea Oceanographic Data Center (KODC) is also used to estimate the EKWC characteristics in details. *P*-vector method is applied to three datasets of KODC, GDEM and

WOA to obtain the current vectors in the East (Japan) Sea.

KODC dataset for the period of 1971 to 1997 is collected and regridded with  $1/10^\circ$  resolution from the hydrographic survey lines from 207 to 101. This is bimonthly hydrographic survey data suitable to get the climatological data (27-year bimonthly mean) as well as for the study of its variability (<http://www.nfrda.re.kr/kodc>).

GDEM is a four dimensional digital model of temperature and salinity for the total basin of the world ocean (Teague *et al.*, 1990). GDEM consists of set of coefficients of mathematical expressions describing vertical profiles of temperature and salinity. High resolution GDEMs have been built for selected areas, such as a region of East/Japan Sea, on  $10' \times 10'$  space grid for each months. The basic design concept of GDEM is the determination of a set of analytical curves that represent the mean vertical distributions of temperature and salinity for grid squares through the averaging of the coefficients of the mathematical expressions for the curves found for individual profiles. Different families of representative curves have been chosen for shallow, mid-depth, and deep ranges. GDEM dataset is currently available on the Internet (<http://128.160.23.42/gdemv/gdemv.html>).

WOA dataset (<http://www.nodc.gov/OC5/>) consists of objectively analyzed fields of temperature, salinity and oxygen. On the high resolution version of WOA (Boyer & Levitus, 1997) objectively analyzed all-data annual mean temperature and salinity fields have been computed on a  $15' \times 15'$  grid, it is comparatively close to the  $10'$  grid step of GDEM.

### P-vector Method

Traditional geostrophic method has been widely used to obtain the baroclinic components of the geostrophic velocity by assuming the level of no motion at chosen depth. The major drawback with this method is that one does not have a priori knowledge of reference level. Techniques (Schott & Stommel, 1978; Wunsch, 1994) have been developed to determine the reference velocity. The *P*-vector method (Chu, 1995, Chu *et al.*, 1998a and 1998b) was developed to overcome such a problem, it provides absolute velocity. Special effort is paid to formulate the inverse problem for the calculation of absolute velocity from the *T-S* data with the ill-condition check-up. The important feature of this method is the direct application of *P*-vectors for estimation of the velocity vector direction. Following is the brief mathematical formulation for the *P*-vector. The potential density,  $\rho$ , and potential vorticity,  $q$ , of each fluid element would be conserved:

$$V \cdot \nabla \rho = 0, \quad V \cdot \nabla q = 0, \quad q \equiv f \frac{\partial \rho}{\partial z}, \quad \nabla \equiv i \frac{\partial}{\partial x} + j \frac{\partial}{\partial y} + k \frac{\partial}{\partial z}, \quad (1)$$

where  $V = (u, v, w)$ , – the velocity;  
 $(x, y, z)$  – the coordinate;  
 $f$  – is the Coriolis parameter.

Pedlosky (1986) pointed out that the three-dimensional velocity field can be determined from knowledge of the density field unless the potential vorticity and density surfaces coincide:

$$\nabla_{\rho} \cdot \nabla_q \neq 0, \quad (2)$$

Under this condition, a unit vector

$$P = \frac{\nabla \rho \times \nabla q}{|\nabla \rho \times \nabla q|} \quad (3)$$

does exist and can be determined by the density field only. The vector  $V$  is perpendicular to both  $\nabla \rho$  and  $\nabla q$ , therefore,  $V \approx \nabla_{\rho} \cdot \nabla_q$ . *P*-vector is parallel to velocity vector  $V$ , so  $V = r(x, y, z)P$ , where  $r(x, y, z)$  is a proportionality. Applying the thermal wind relation to any two different depths  $z_k$  and  $z_m$ , a set of algebraic equations for determining the parameter  $r$  is obtained. If  $N$  is a total number of levels, there are  $(N-1)$  sets of equations for computing  $r^{(k)}$  for a given level  $z=z_k$ . All these  $(N-1)$  sets of equations are compatible under the thermal wind constraint and should provide the same solution. However, due to errors in measurements and computations, the parameter  $r^{(k)}$  may vary with  $m$ . Least-squares method is applied to minimize the error.

Consistent with geostrophy,  $P$ -vector is assumed to be non-dissipative. Thus it does not incorporate turbulent mixing. The method seems to be valid where geostrophy holds strong with negligible surface and bottom stresses.

## Results

The results of the current vector estimate from GDEM and WOA for the entire East Sea datasets are presented in Fig. 1 and 2. The Figures are arranged to show the horizontal distributions of annual mean, winter (February) and summer (August) month current vectors at surface and 200 m depth. For the southwestern part of the East Sea, the current vector estimates are shown in Fig. 3, 5, and 7 where annual mean and winter and summer cases at surface and 200 m depth are depicted. In Fig. 3, 6, and 8, cross-sectional distribution along 129.9°E with northward velocity components are shown to illustrate the details of the EKWC and the Ulleung Warm Eddy structures. In particular, the results for the year of 1997 are presented to illustrate the pronounced variability of the EKWC in Fig. 7. All Figures are with density background.

Fig. 1a-f show the current vector distributions for annual mean, winter and summer cases. The circulation patterns represent tow gyre system; in the north of the polar front situated between 39 and 40°N, cyclonic gyre exists while in the south anticyclonic gyre system is developed. They are in good agreement with traditional views (Uda, 1934; Moriyasu, 1972). However, our results represent vigorous mesoscale eddy activities on the entire domain. Fig. 1b and 1c can be compared to show the seasonal variation in terms of may features such as amplitude of the meandering axis of the polar front, number of mesoscale eddies, intensity of the major current such as TWC, EKWC, NKCC, and Liman/Primorye.

Fig. 2 shows the current vectors estimated by using WOA dataset for the annual mean only. The WOA has broader horizontal resolution than that of GDEM and is averaged over the entire month. As a matter of fact, they represent much smoother field with reduced eddy activities and meandering of the polar frontal axis. However, it shows the general circulation pattern in that EKWC and Ulleung eddy is well reproduced. The southwestern part of the East Sea deserves a closer look, since it is the region for the EKWC and Ulleung warm eddy shown in Fig 3. Three datasets commonly reproduce reasonably well the EKWC and mesoscale Ulleung warm eddy. In detail, they reveal the differences in the intensity of the current and the characteristics of the eddy. In addition, the KODC dataset reveal the most important feature that the southward undercurrent is developed beneath the northward EKWC. To facilitate the view of undercurrent, Fig. 4, 6, and 8 are presented where cold and denser water originated from north is subducted into the south and flowing with speed greater than 10 cm/sec between 100–200 meter depths. This is a striking result which have been long suspected, but failed to reveal (Kim & Kim, 1983). The undercurrent in summer season is getting stronger with the increased surface northward current in Fig. 8 compared to winter season in Fig. 6. This is very analogous to two-layer estuarine circulation pattern where in upper layer, the flow is directed toward open sea and in the lower layer, the flow is directed to the head of estuary.

To illustrate the year-to-year variability of the EKWC, Fig. 5-8 are presented in that we compare the 27-year mean current vectors and that of 1997. It should be indicated that the EKWC is in strong interaction with the Ulleung Warm Eddy so that with regard to the formation of this Eddy, the intensity and flow patterns of the EKWC is changing significantly. Of course, the undercurrent from the north is also significantly changing. The results of current vector estimates comparison between GDEM, WOA and KODC are summarized in Table 1.

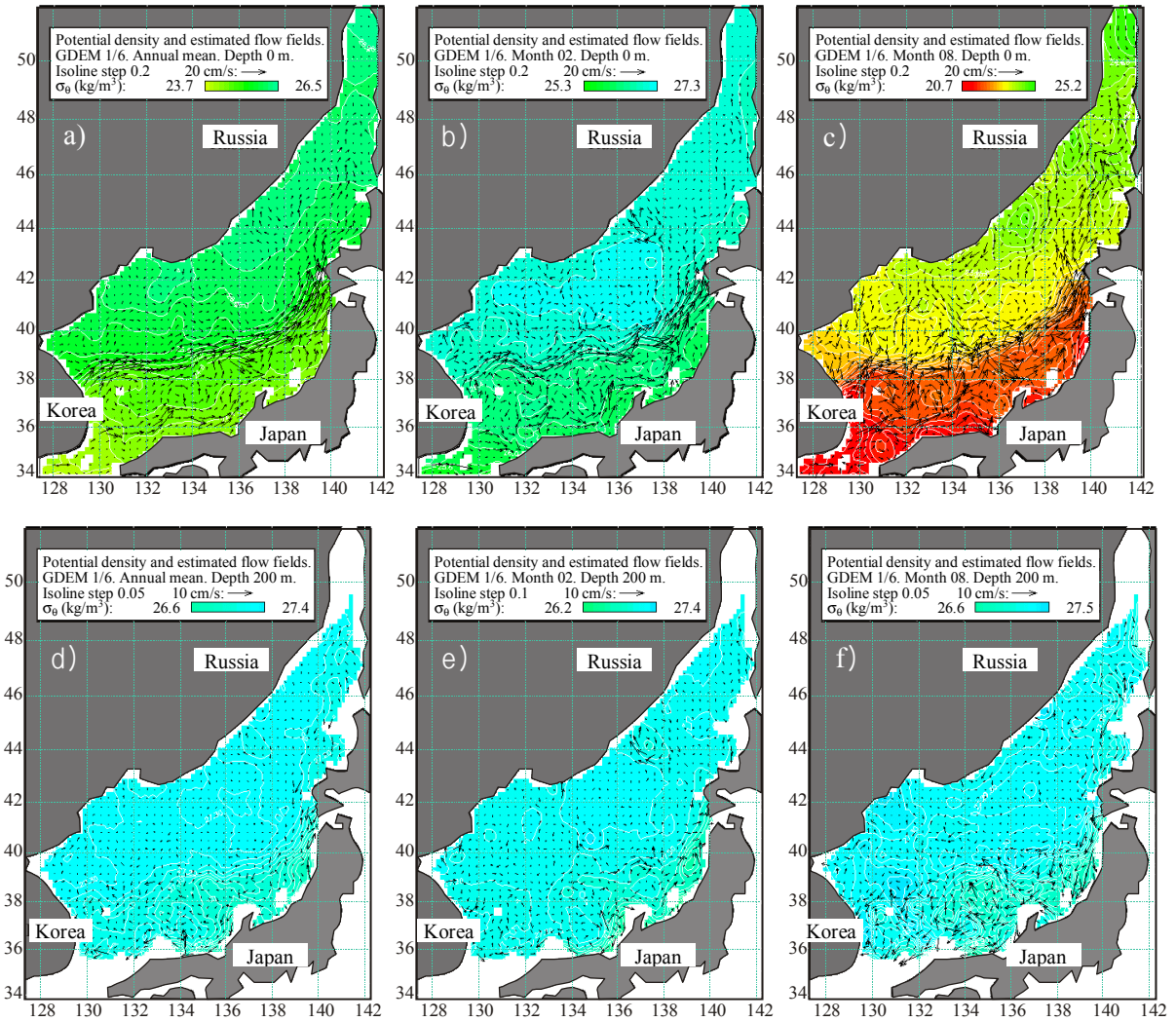


Fig. 1. Horizontal distribution of current vector estimates using the GDEM dataset. Left: Annual mean (a,d), Middle: February (b, e), Right: August (c, f). Upper: Depth 0 m (a-c), Lower: Depth 200 m (d-f)

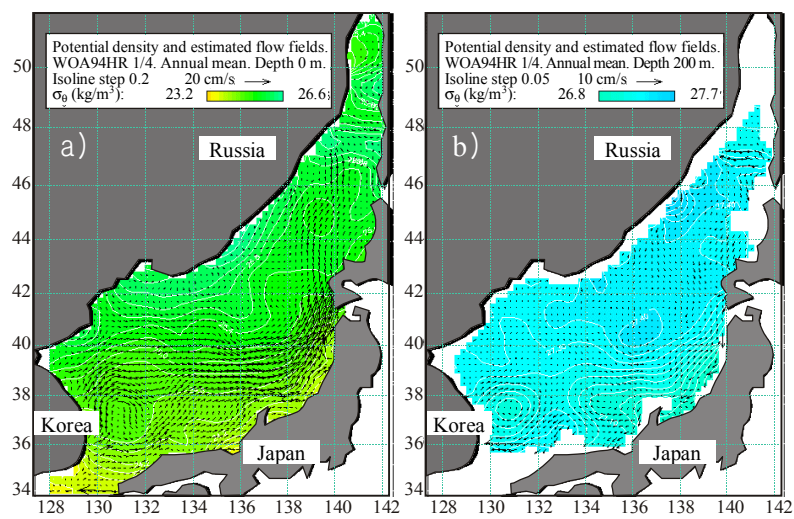


Fig. 2. Horizontal distribution of current vector estimates using the WOA-94 dataset. Left: Depth 0m (a), Right: Depth 200 m (b)

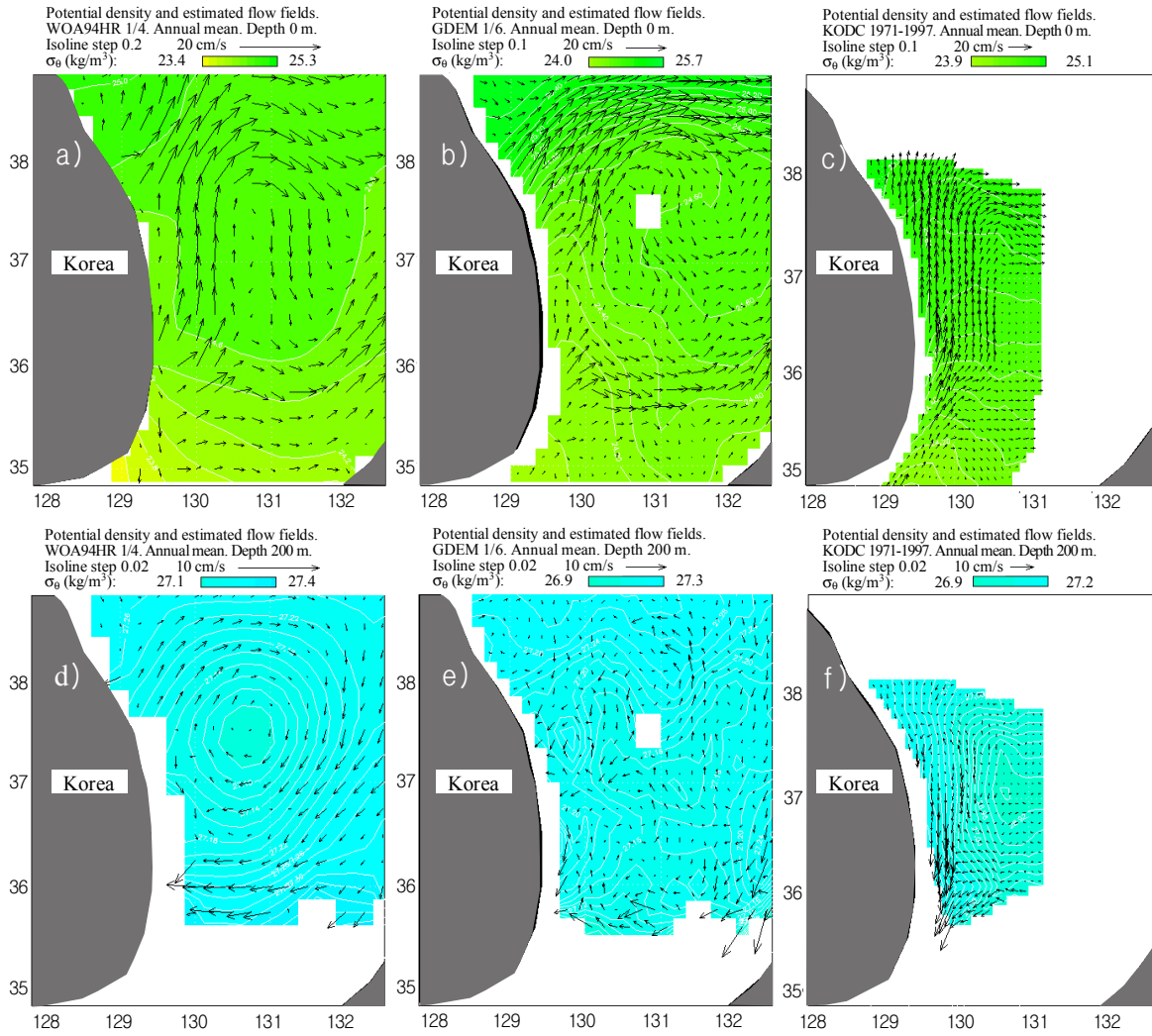


Fig. 3. Horizontal distribution of annual mean current vector estimates using three datasets. Left: WOA-94 (a,d), Middle: GDEM (b, e), Right: KODC (c, f). Upper: Depth 0 m (a-c), Lower: Depth 200 m (d-f)

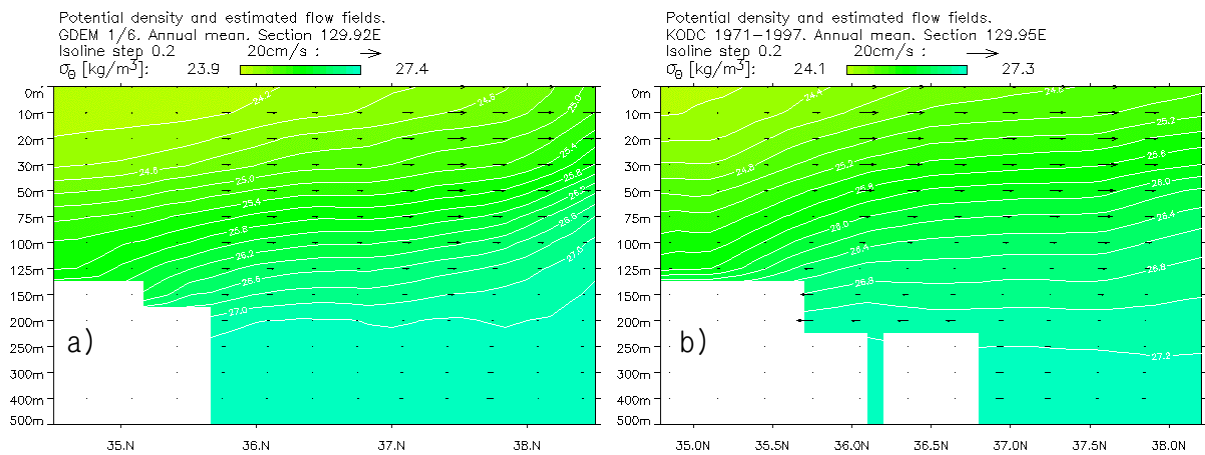


Fig. 4. Meridional cross-section of annual mean current vector estimates along 129.9 E using GDEM and KODC datasets. Left: GDEM (a), Right: KODC (b)

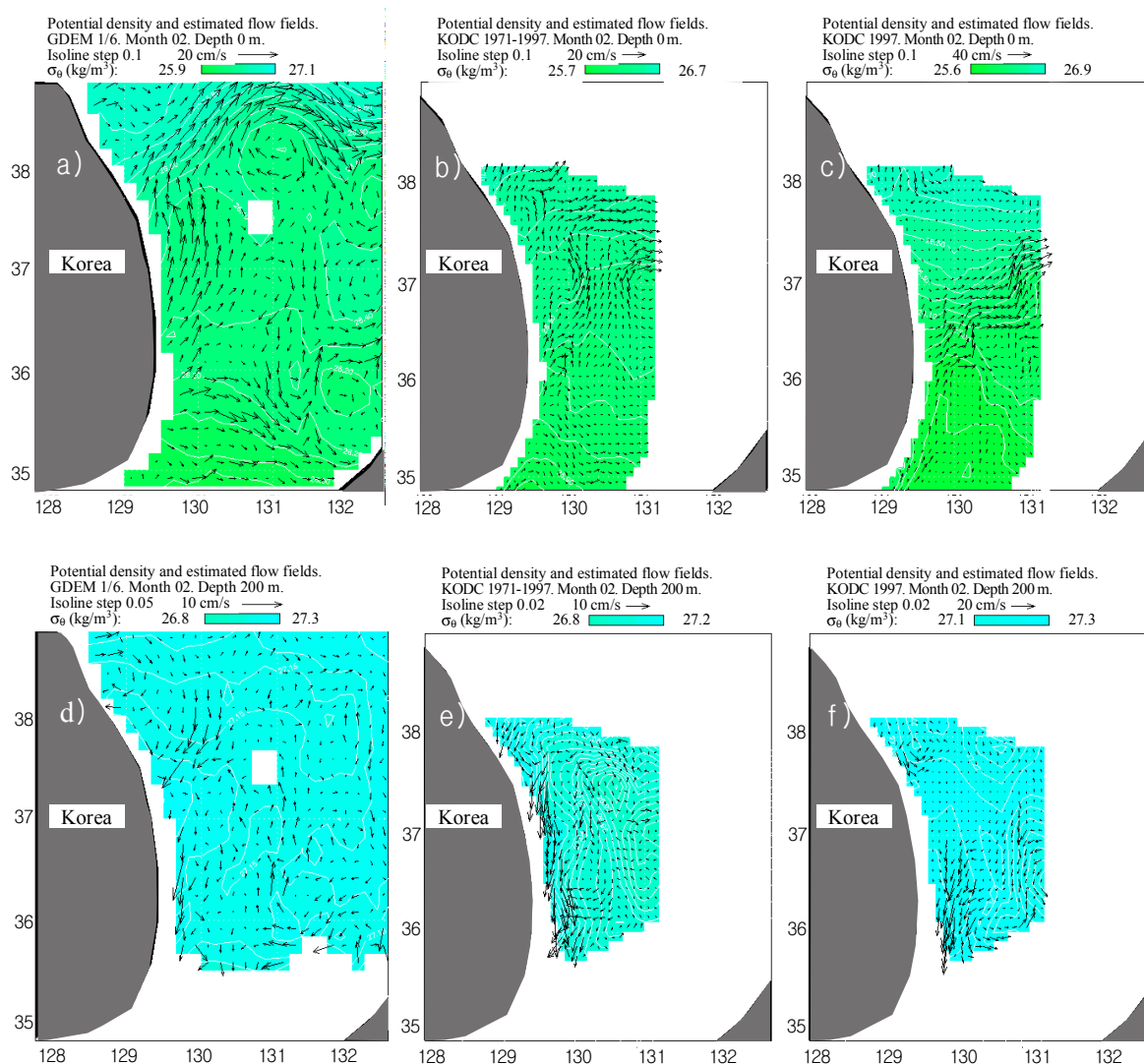


Fig. 5. Horizontal distribution of current vector estimates for February using GDEM and KODC datasets. Left: GDEM (a, d), Middle: KODC climatology 1971-1997 (b, e), Right: KODC 1997 (c, f). Upper: Depth 0 m (a-c), Lower: Depth 200 m (d-f)

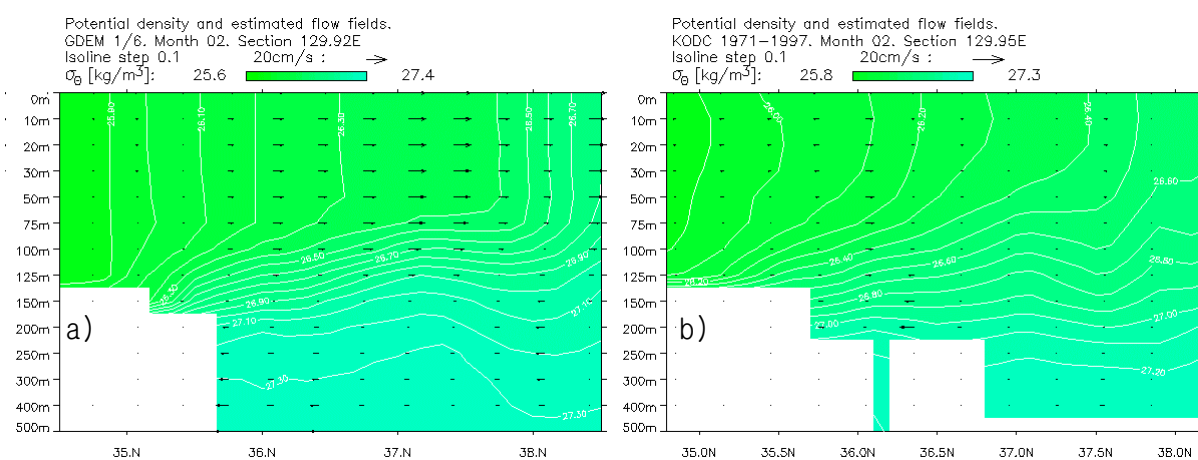


Fig. 6. Meridional cross-section of current vector estimates along 129.9N for February using GDEM and KODC datasets. Left: GDEM (a), Right: KODC (b).

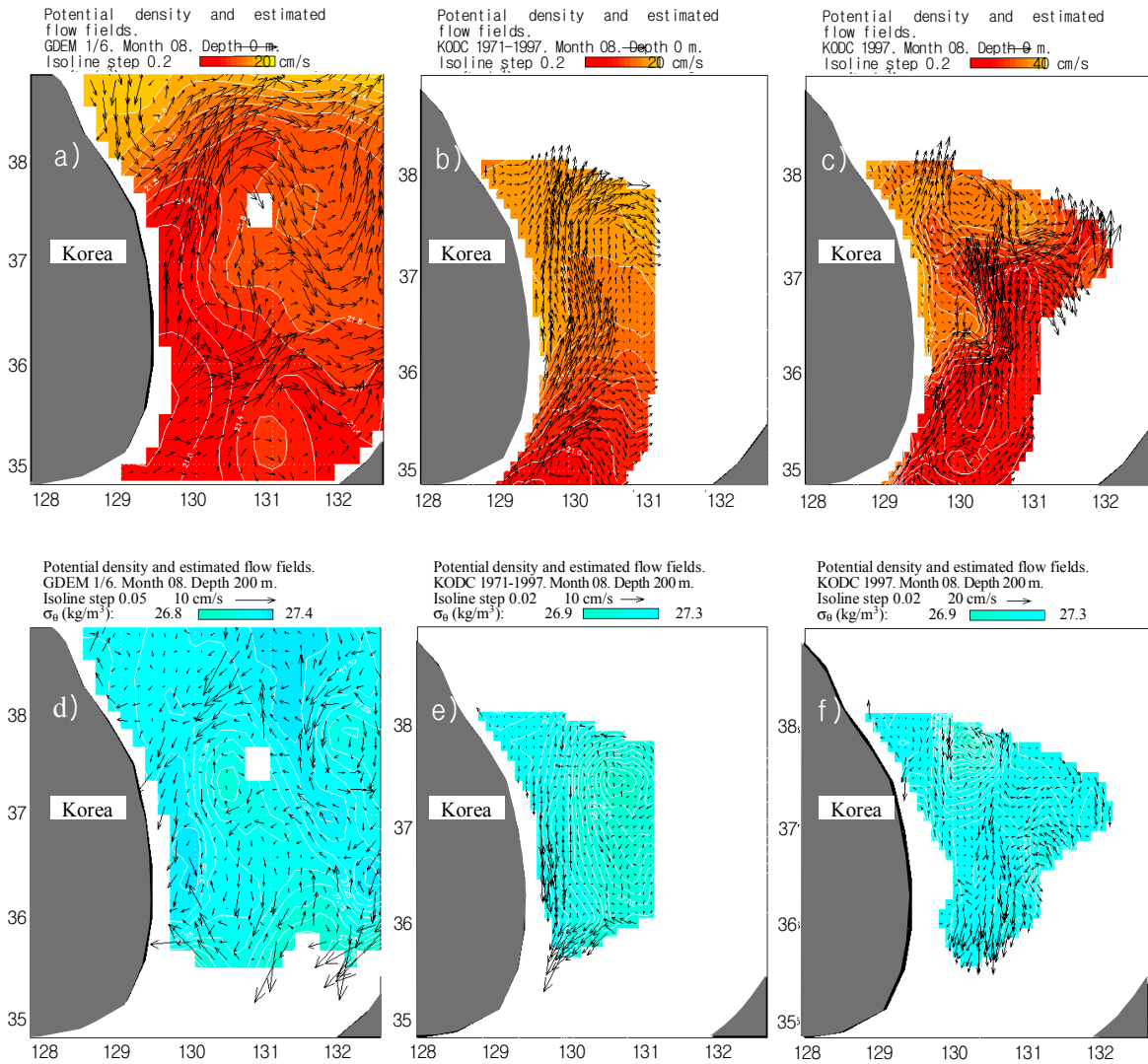


Fig. 7. Horizontal distribution of current vector estimates for August using GDEM and KODC datasets. Left: GDEM (a,d), Middle: KODC climatology 1971-1997 (b, e), Right: KODC 1997 (c, f). Upper: Depth 0 m (a-c), Lower: Depth 200 m (d-f)

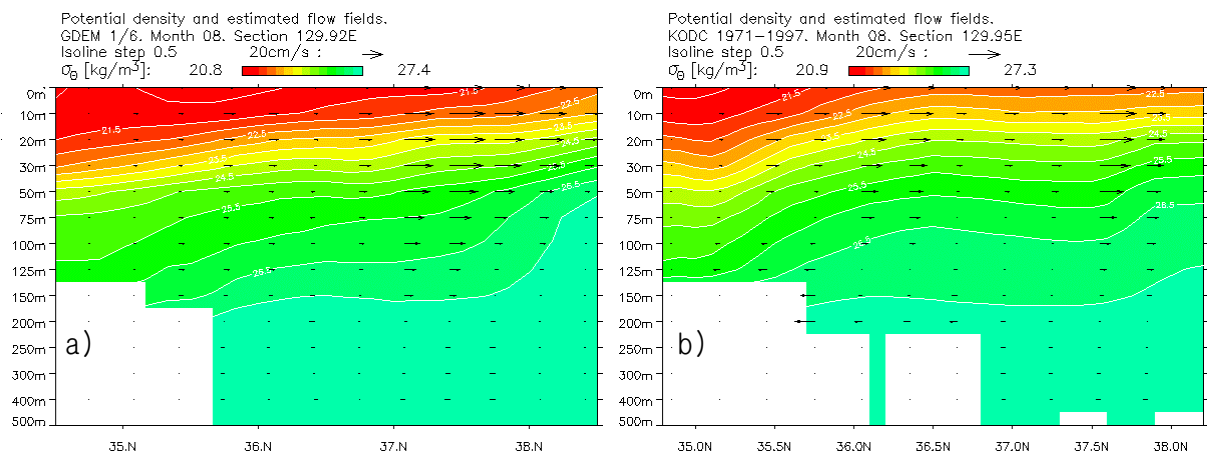


Fig. 8. Meridional cross-section of current vector estimates along 129.9 N for August using GDEM and KODC climatology datasets. Left: GDEM (a), Right KODC (b)

Table 1

*Results of the current vector estimates by P-vector method for the East Sea*

Dataset / Time Frame	Section	Fig. N	Results
GDEM / Annual mean	Surface	1a, 3b	TWC is well reproduced with Polar Frontal jet. Weak EKWC (about 4 cm/s) near 36.5°N. Ulleung warm anticyclonic eddy. Weak flow in the shallow region of Korea Strait.
	Horizon 200 m	1d, 3e	Undercurrents of Polar Front jet and TWC.
	Section 129.9°N	4a	Insignificant undercurrent of EKWC.
GDEM / February	Surface	1b, 5a	Shows well the general circulation pattern. TWC, EKWC and Polar Front jet are well reproduced (velocities about 15-20 cm/s). More spatial structures due to local eddy activities. Northward water movement in NKCC area. Strong anticyclonic eddy in the Primorye area. Southward propagation on the region about (130°E, 40°N). Weak flow in the shallow region of Korea Strait.
	Horizon 200 m	1e, 5d	Undercurrents of TWC and of EKWC. No distinct undercurrent of Polar Front jet. Strong anticyclonic eddy in the Primorye area.
	Section 129.9°N	6a	Undercurrent of EKWC.
GDEM / August	Surface	1c, 7a	Shows well the general circulation pattern. Much more eddy activities with a strong meandering of polar front. TWC, EKWC, Polar Front jet and NKCC are reproduced well. Strong Ulleung warm anticyclonic eddy. Northward flow in a wide region about (130°E, 40°N). Southward flow directly from Primorye area to Polar Front jet area.
	Horizon 200 m	1f, 7d	Strong undercurrents (about 5 cm/s) of Polar Front jet, TWC, EKWC and NKCC.
	Section 129.9°N	8a	Deep undercurrent between 37°N and 38°N
WOA / Annual mean	Surface	2a, 3a	EKWC is reproduced well, maximal velocity about 8 cm/s. Other features are similar to GDEM, but with less spatial resolution and highly smoothed. Overshooting of Polar Front jet up to 40N on western part of East Sea. Frontal jet is wide, with a maximal velocities about 10-12 cm/s. Weak flow in the shallow region of Korea Strait.
	Horizon 200 m	2b, 3d	Ulleung Warm eddy is well reproduced. Centered on (130.8°E 37.5°N). Maximal velocities about 2 cm/s. Undercurrent of TWC, no undercurrent of Polar Front jet.
KODC 1971-1997 / Annual mean	Surface	3c	Strong EKWC (about 25-30 cm/sec). Weak flow in the shallow region of Korea Strait.
	Horizon 200 m	3.f	Southward cold current intrusion
	Section 129.9°N	4b	Undercurrent of EKWC from 37.5°N to 36°N.
KODC 1971-1997 / February	Surface	5b	EKWC is reproduced well. Small scale eddies in UB area.
	Horizon 200 m	5e	Southward cold current intrusion alongshore.
	Section 129.9°N	6b	Undercurrent of EKWC from 37.5°N to 36°N.
KODC 1971-1997 / August	Surface	7b	Strong EKWC, TWC (about 30 cm/s) and Ulleung warm eddy.
	Horizon 200 m	7e	Undercurrent (about 10 cm/s) of EKWC from 37.5°N to 36°N. Non significant flow of UB eddy. Overestimated undercurrent in the Korea Strait shallow region.
	Section 129.9°N	8b	Undercurrent of EKWC from 37.5°N to 36°N. Strong undercurrent of EKWC.
KODC 1997 / February	Surface	5c	EKWC is reproduced (about 30 cm/s), the position of TWC is quite different from 1971-1997 climatology.
	Horizon 200 m	5f	Undercurrent of EKWC from 37°N to 36°N. Overestimated undercurrent in the Korea Strait shallow region.
KODC 1997 / August	Surface	7c	Strong EKWC and TWC flow (about 50 cm/s) with a high spatial variability due to small scale eddies. EKWC is deviated from Korean coastline at 36.4°N up to 130.5°E, due to the intrusion of a cold water.
	Horizon 200 m	7f	Undercurrent of EKWC with a velocities about 10 cm/s from 37.5°N to 36°N. Overestimated undercurrent in the Korea Strait shallow region.

## Discussion and Summary

The current vectors estimated by P-vector shows realistic general circulation patterns which agree with traditional schemes of circulation in the East Sea (Uda, 1934; Moriyasu, 1972). In details, they reproduced major currents such as TWC, EKWC, and NKCC. The EKWC is associated with the most pronounced feature, polar frontal jet. Mesoscale eddies are well reproduced in the recognizable locations such as Ulleung and Yamato Basins and *etc.* It is clearly noticeable even in the climatological datasets to show the seasonal variability from winter to summer. The seasonal variation can be fully appreciated in examining the occurrences of the mesoscale eddies and meandering of the polar front jet axis.

In comparing the annual mean current vectors estimates from GDEM and WOA datasets, they agree with each other on the whole. In inspecting the details of the major current intensities, they exhibit considerable differences. The current field from WOA is smooth while in the GDEM, it shows much more active mesoscale eddy activities with pronounced meandering features of polar front in the East Sea. Both datasets reproduce the EKWC clearly enough but with different intensity.

The P-vector method is simple and clear, while it has some limitations. First the estimates in the surface and bottom boundary layers are unrealistic results, particularly in the shallow regions. Second, in the regions where barotropic process is more important due to strong vertical mixing, the estimates seem unrealistic.

## References

1. Boyer T.P. & Levitus S. 1997. Objective analyses of temperature and salinity for the world ocean on a 1/4 degree grid. NOAA Atlas NESDIS 11.
2. Chu P.C. 1995. P vector method for determining absolute velocity from hydrographic data // J. Mar. Technol. Soc. Vol. 29. N 3. P. 3-14.
3. Chu P.C., Fan C.W. & Cai W.J. 1998b: P-vector inverse method evaluated using the Modular Ocean Model (MOM) // J. Oceanography. Vol. 54. P. 185-198.
4. Chu P.C., Lozano C.J. & Kerling J.L. 1998a. An airborne expendable bathythermograph survey of the South China Sea, May 1995 // J. Geophysical Research. Vol. 103. N C10. P. 21637-21652.
5. Hase H., Yoon J.-H., Takematsu M., Koterayama W. & Yamaguchi S. 1997. The structure of the Tsushima Warm current off the Wakasa bay during 1995-96 // Engineer. Sci. Rep. Kyushu Univ. N 19. P. 61-66.
6. Kang H.S. 1997. Implementation, sensitivity testing, and evaluation of a numerical model for the East/Japan Sea Circulation / MS thesis. Univ. of Miami. USA. 174 pp.
7. Kawabe M. 1982a. Branching of the Tsushima Current in the Japan Sea. Part I: Data analysis // J. Oceanography Society. Vol. 38. P. 95-107.
8. Kawabe M. 1982b. Branching of the Tsushima Current in the Japan Sea, Part II: Numerical experiment // J. Oceanography Society. Vol. 38. P. 183-192.
9. Kim C.H. & Kim K. 1983. Characteristic and origin of the cold water mass along the east coast of Korea // J. Oceanol. Soc. Korea. Vol. 18. P. 73-83.
10. Kim C.-H. & Yoon J.-H. 1996. Modeling of the wind-driven circulation in the Japan Sea using a reduced gravity model // J. Oceanography. Vol. 52. P. 359-373.
11. Kim C.-H. 1996. A numerical experiment study on the circulation of the Japan Sea (East Sea) / Ph. D. thesis. Kyushu Univ. 151 pp.
12. KORDI 1987. On the understanding of dynamical Processes of the circulation in the southeastern part of the East Sea / BSPE 00083-147-1.
13. KORDI 1999. Variability of basin-to-basin water exchanges in the East Sea. BSPE 99756-00-1241-1. 217 pp.
14. Kuh K. & Legekis R., 1987. Branching of the Tsushima Current in 1981-83 // Progress in Oceanography. N 17. P. 265-276.
15. Moriyasu S. 1972. The Tsushima Current / In Kuroshio – Its physical Aspects. Ed. Stommel H. & Yoshida K. Univ. Tokyo. Japan. P. 353-369.
16. Pedlosky J. 1986. Thermocline theories / General Circulation of the Ocean. Ed. Abardanel H.D.I. & Young W.R. New York: Springer-Verlag. P. 55-101.
17. Ro Y.J. 1999a. Numerical Experiments of the Mesoscale Eddy Activities in the East (Japan) Sea // Proc. CREAMS'99. Fukuoka. Japan. P. 116-120.
18. Ro Y.J. 1999b. Numerical modeling of the Meso-scale Eddies in the East (Japan) Sea // J. Korean Soc. of Oceanogr. (in press)
19. Ro Y.J. 2000. Numerical Modelling Experiments of the East (Japan) Sea Circulation and Mesoscale Eddy Generations based on POM-ES // Proc. 6<sup>th</sup> Estuarine and Coastal Modeling Conference. New Orleans. USA.
20. Schott F. & Stommel H. 1978. Beta spirals and absolute velocities in different oceans // Deep Sea Res. Vol. 25.

- P. 961-1010.
21. Sekine Y. 1991. A numerical experiment on the seasonal variation of the oceanic circulation in the Japan Sea / *Oceanography of Asian Marginal Seas*. Ed. Takano K. Elsevier Oceanography Series. Vol. 54. P. 113-128.
  22. Seung Y.H. & Nam S.Y. 1992b. A numerical study on the barotropic transport of the Tsushima Warm Current // *La mer*. Vol. 30. P. 139-147.
  23. Seung Y.H. 1992a. A simple model for separation of East Korean Warm Current and formation of the North Korean Cold Current // *J. Oceanol. Soc. Korea*. Vol. 27. P. 189-196.
  24. Takematsu M., Ostrovskii A.G. & Kitamura T. 1994. Current feature in the Japan Sea's proper water // *Third CREAMS Workshop*. Seoul. Korea. P. 1-4.
  25. Teague W.J., Carron M.J. & Hogan P.J. 1990. A comparison between the Generalized Digital Environmental Model and Levitus climatologies // *J. Geophysical Research*. Vol. 95. N C5. P. 7167-7183.
  26. Uda M. 1934. The result of simultaneous oceanographical investigation in the Japan Sea and its adjacent waters in May and June, 1932 // *J. Imp. Fish. Exp. Sta.* Vol. 5. P. 57-190.
  27. UNESCO 1981. Tenth report of the joint panel on oceanographic tables and standards. UNESCO Tech. Papers in Marine Science. N 36. Paris: UNESCO.
  28. Wang K., Fang G. & Ro Y.J. 1999. Barotropic Numerical Studies on the driving mechanism of the East Korea Warm Current // *Studia Marina Sinica*. Vol. 41.
  29. Wunsch C. 1994. Dynamically consistent hydrography and absolute velocity in the eastern North Atlantic Ocean // *J. Geophysical Research*. Vol. 99. P. 14071-14090.
  30. Yoon J.H. 1982a. Numerical experiment on the circulation in the Japan Sea. Part 1: Formation of the East Korean Warm Current // *J. Oceanography Society, Japan*. Vol. 38. P. 43-51.
  31. Yoon J.H. 1982b. Numerical experiment on the circulation in the Japan Sea. Part 3: Formation of the nearshore branch of the Tsushima Current // *J. Oceanography Society, Japan*. Vol. 38. P. 119-124.
  32. Yurasov G. & Yarichin B.G. 1991. Currents of the Japan Sea. Vladivostok: FEB, Academy of Science, USSR. 176 pp.